


RESEARCH

Open Access



Blockade of the mitochondrial DNA release ameliorates hepatic ischemia-reperfusion injury through avoiding the activation of cGAS-Sting pathway

Yi Xiong^{1†}, Jiawen Chen^{1†}, Wei Liang^{1†}, Kun Li², Yingqi Huang¹, Jingwen Song¹, Baoyu Zhang³, Xiusheng Qiu⁴, Dongbo Qiu^{4*}, Qi Zhang^{1,4*} and Yunfei Qin^{1,4*} 

Abstract

Background Liver surgery during the perioperative period often leads to a significant complication known as hepatic ischemia-reperfusion (I/R) injury. Hepatic I/R injury is linked to the innate immune response. The cGAS-STING pathway triggers the activation of innate immune through the detection of DNA within cells. Nevertheless, the precise mechanism and significance of the cGAS-STING pathway in hepatic I/R injury are yet to be investigated.

Methods Mouse model of hepatic I/R injury was used in the C57BL/6 WT mice and the STING knockout (STING-KO) mice. In addition, purified primary hepatocytes were used to construct oxygen-glucose deprivation reperfusion (OGD-Rep) treatment models.

Results Our research revealed a notable increase in mRNA and protein levels of cGAS and STING in liver during I/R injury. Interestingly, the lack of STING exhibited a safeguarding impact on hepatic I/R injury by suppressing the elevation of liver enzymes, liver cell death, and inflammation. Furthermore, pharmacological cGAS and STING inhibition recapitulated these phenomena. Macrophages play a crucial role in the activation of the cGAS-STING pathway during hepatic I/R injury. The cGAS-STING pathway experiences a significant decrease in activity and hepatic I/R injury is greatly diminished following the elimination of macrophages. Significantly, we demonstrate that the activation of the cGAS-STING pathway is primarily caused by the liberation of mitochondrial DNA (mtDNA) rather than nuclear DNA (nDNA). Moreover, the safeguarding of the liver against I/R injury is also attributed to the hindrance of mtDNA release through the utilization of inhibitors targeting mPTP and VDAC oligomerization.

[†]Yi Xiong, Jiawen Chen, and Wei Liang equal contributions to this work.

*Correspondence:
Dongbo Qiu
qjudb3@mail.sysu.edu.cn
Qi Zhang
keekee77@126.com
Yunfei Qin
qinyf6@mail.sysu.edu.cn

Full list of author information is available at the end of the article



© The Author(s) 2024. **Open Access** This article is licensed under a Creative Commons Attribution-NonCommercial-NoDerivatives 4.0 International License, which permits any non-commercial use, sharing, distribution and reproduction in any medium or format, as long as you give appropriate credit to the original author(s) and the source, provide a link to the Creative Commons licence, and indicate if you modified the licensed material. You do not have permission under this licence to share adapted material derived from this article or parts of it. The images or other third party material in this article are included in the article's Creative Commons licence, unless indicated otherwise in a credit line to the material. If material is not included in the article's Creative Commons licence and your intended use is not permitted by statutory regulation or exceeds the permitted use, you will need to obtain permission directly from the copyright holder. To view a copy of this licence, visit <http://creativecommons.org/licenses/by-nc-nd/4.0/>.

Conclusions The results of our study suggest that the release of mtDNA plays a significant role in causing damage to liver by activating the cGAS-STING pathway during I/R injury. Furthermore, inhibiting the release of mtDNA can provide effective protection against hepatic I/R injury.

Keywords cGAS, Hepatic ischemia-reperfusion injury, Innate immunity, mtDNA, STING

Introduction

During liver surgeries, hepatic I/R injury is a frequently observed pathophysiological occurrence in the perioperative period [1]. Based on various clinical scenarios, hepatic I/R injury can be divided into warm hepatic I/R injury or cold hepatic I/R injury. Most hepatic I/R injuries are warm hepatic I/R injuries, which are related to the liver surgeries mentioned above and initiated by hepatocyte damage. Hepatic I/R injury in a cold environment happens exclusively when organs are stored at low temperatures before liver transplantation. During this injury, hepatic sinusoidal endothelial cells are damaged and microcirculation in the liver is disrupted [2, 3]. Hepatic I/R damage may lead to elevated transaminases, biliary strictures, dysfunction of the transplanted organ, and both acute and long-term rejection [4]. Severe liver I/R damage may result in elevated rates of mortality and morbidity [5–7].

The processes involved in hepatic I/R damage are quite intricate. Although intensively studied for several decades, the comprehensive mechanisms are still not adequately uncovered. Nevertheless, hepatic I/R injury encompasses a dual stage. The ischemia phase directly causes liver cell damage, and the reperfusion phase leads to continuous liver cell damage related to inflammation [8]. Reactive oxygen species (ROS), mitochondrial DNA (mtDNA), intracellular calcium overload, Kupffer cells (KCs), neutrophils, and various cytokines and chemokines are the primary elements contributing to hepatic I/R injury [9]. In recent times, it has become more and more evident that the sterile innate immune reaction plays a critical role in hepatic I/R damage [10].

The liver, being a major immune organ, is abundant in diverse innate immune cells [11]. In response to signals of pathogens or damaged cells or tissues, liver innate immune cells can be activated to triggers an innate immune response, eliciting an inflammatory reaction [12, 13]. Activation of DNA triggers the cGAS-STING signaling pathway, which is a crucial signaling cascade of the innate immune system. In the past, the cGAS-STING signaling pathway was primarily believed to have a crucial function in innate immunity and protecting the host [14]. Our previous studies [15–18] have shown that the cGAS-STING pathway is strongly associated with liver diseases, such as MAFLD, abnormal lipid metabolism, and liver cancer. Nonetheless, the precise involvement of the cGAS-STING pathway in hepatic I/R damage remains uncertain. Further investigation is required to analyze the

intricate mechanism, as recent research has suggested that hepatic I/R injury is influenced by the excitation of the cGAS-STING signaling pathway [19].

This research showcased the upregulation of cGAS and STING, along with the significant activation of the cGAS-STING signaling pathway, in hepatic I/R injury. The lack of STING provided significant protection against hepatic I/R damage. After the removal of liver macrophages, which are recruited and activated during hepatic I/R injury, we observed a notable reduction in the strength of the cGAS-STING signaling pathway activation. This reduction plays a crucial role in safeguarding the liver against I/R injury. Pharmacologically, the alleviation of hepatic I/R injury can also be achieved by inhibiting cGAS and STING. Furthermore, we discovered that serum mitochondrial DNA was markedly increased in hepatic I/R injury. By employing medications, we suppressed the release of mtDNA and observed a concomitant decrease in the activity of the cGAS-STING pathway. Additionally, these inhibitors have demonstrated their ability to safeguard the liver from damage caused by ischemia-reperfusion. Finally, we evaluated the safety of all of these inhibitors. The results of our study indicate that the cGAS-STING pathway is clearly triggered during hepatic I/R injury, and suppressing its activation emerges as a crucial approach for the prevention and treatment of hepatic I/R injury.

Results

Hepatic I/R injury triggers the activation of the cGAS-STING signaling pathway

In order to investigate the association between the cGAS-STING pathway and hepatic I/R injury, we initially conducted a sham procedure followed by inducing 70% warm hepatic I/R injury in mice of the wide type genotype. After reperfusion, serum and liver samples were collected at the 6-hour mark to evaluate liver damage using serum ALT and AST (Fig. 1A-B) levels, as well as H&E staining (Fig. 1C). TUNEL staining was used to evaluate hepatocyte apoptosis in liver injury induced by I/R. After reperfusion, there was a notable rise in the quantity of TUNEL-positive cells, as depicted in Fig. 1D. Consistent with previous studies, I/R sera showed obviously increased liver transaminases, and I/R livers showed hepatocellular necrosis, edema, and sinusoidal congestion compared to sham sera and livers.

During hepatic I/R injury, the detection process involved identifying important components like cGAS,

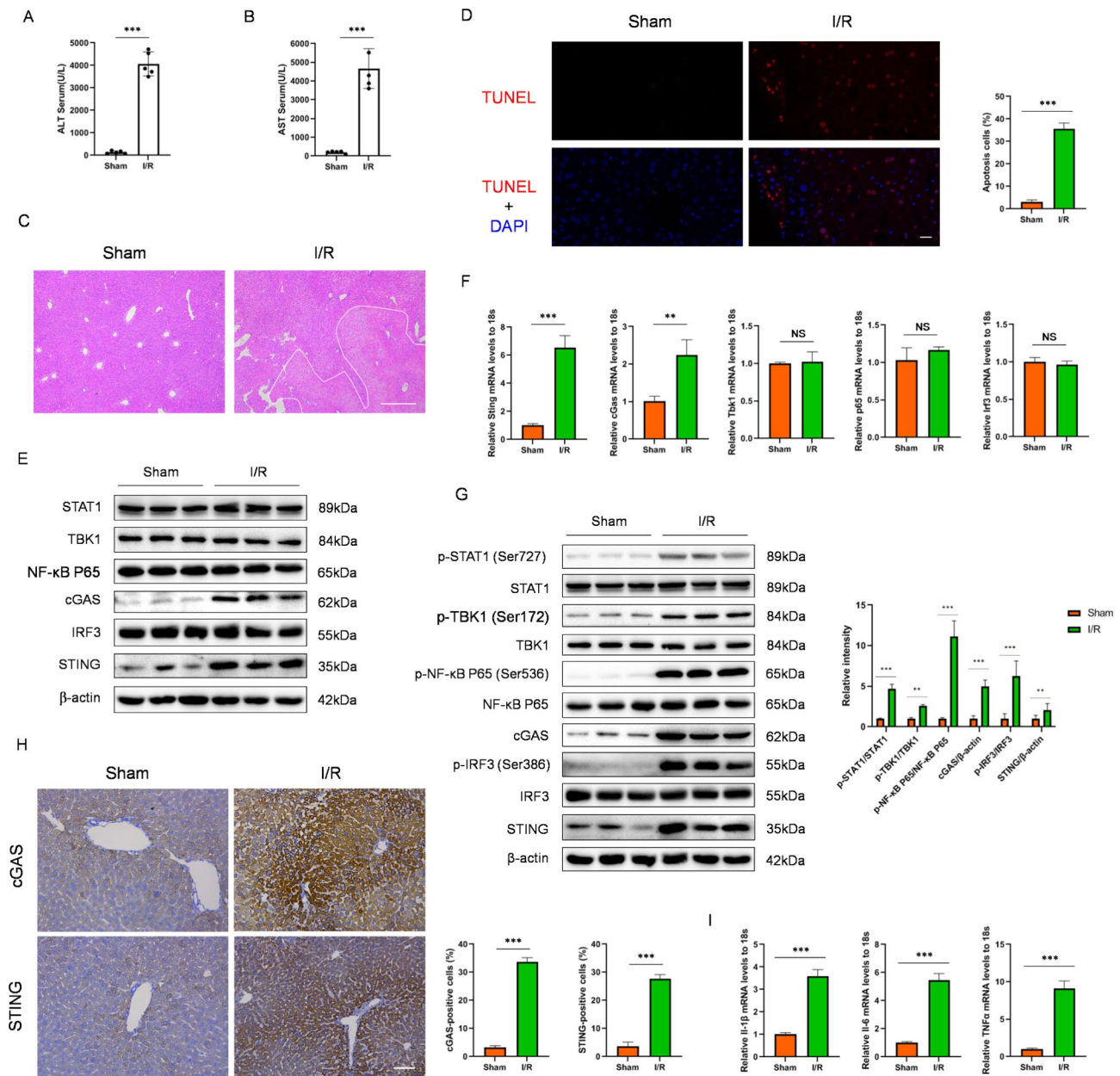


Fig. 1 Activation of the cGAS-STING pathway is associated with hepatic I/R injury in mice. **(A-B)** Serum ALT/AST activities from mice subjected to sham or ischemia treatment for 1.5 h, followed by reperfusion for 6 h ($n=5$ per group). **(C)** Representative image of H&E stained liver tissues of sham and I/R-treated mice ($n=3$ per group). Scale bar, 250 μm . **(D)** Representative image of TUNEL staining in liver sections from mice with hepatic I/R surgery ($n=3$ per group). Scale bar, 25 μm . **(E)** Protein levels of the p-STAT1, p-TBK1, p-P65, p-IRF3, cGAS and STING in liver tissue of sham and I/R-treated mice detected by immunoblotting. β -actin served as the loading control ($n=3$ per group). **(F)** mRNA expression levels of cGAS, STING, TBK1, P65 and IRF3 in liver tissue of sham and I/R-treated mice were detected by qRT-PCR analysis. **(G)** IHC staining of cGAS and STING in liver tissue of sham and I/R-treated mice ($n=3$ per group). Scale bar, 50 μm . **(H)** Examining the activation of the cGAS-STING pathway by western blotting for phosphorylated STAT1 (p-STAT1)/STAT1, phosphorylated TBK1 (p-TBK1)/TBK1, phosphorylated P65 (p-P65)/P65, phosphorylated IRF3 (p-IRF3)/IRF3, cGAS and STING in liver tissue of sham and I/R-treated mice. β -actin served as the loading control ($n=3$ per group). **(I)** mRNA expression levels of proinflammatory factors (Il1 β , Il6, and Tnfa) in liver tissue of sham and I/R-treated mice were detected by qRT-PCR analysis. Levels of statistical significance are indicated as: * $p < 0.05$, ** $p < 0.01$, *** $p < 0.001$

STING, TBK1, IRF3, P65, and STAT1 within the cGAS-STING pathway during hepatic I/R injury. After hepatic I/R injury, it was observed that solely cGAS and STING exhibited significant upregulation at the protein or mRNA level (Fig. 1E-F), which is consistent with previous

study [20]. Furthermore, the immunohistochemical (IHC) analysis demonstrated a substantial increase in the size of both cGAS-positive and STING-positive regions within the I/R group, as depicted in Fig. 1G. Given that cGAS and STING are also genes stimulated by

interferon [21], we hypothesized that the relevant pathways of innate immunity might be triggered following hepatic I/R injury. As expected, the phosphorylation of TBK1, P65, IRF3 and STAT1 was augmented in I/R livers (Fig. 1H-I). Moreover, it was discovered that certain inflammatory markers, including IL1 β , IL6, and TNF α , exhibited increased expression following the occurrence of an injury (Fig. 1J). In addition, we also found in some human clinical samples that apoptosis of hepatocytes was increased, and the expressions of cGAS and STING are also significantly upregulated (Figure S1A-B and Supplementary table). To summarize, these findings indicate that the levels of cGAS or STING expression was markedly up-regulated, leading to a substantial increase in the activation of cGAS-STING induced innate immune pathways factors during hepatic I/R injury.

The absence of STING alleviates hepatic I/R injury

In order to assess the significance of the cGAS-STING pathway in hepatic I/R injury, we utilized STING-Knockout (KO) mice to examine different markers of hepatic I/R injury. At 6 h after liver I/R surgery (Fig. 2A-B), STING-KO mice displayed reduced levels of ALT and AST compared to WT mice. In STING-KO mice (Fig. 2C-D), liver specimens were analyzed using H&E analysis and TUNEL staining, revealing decreased necrotic regions and apoptosis. Consistent with expectations, the levels of p-TBK1, p-P65, p-IRF3, and p-STAT1 in mice lacking STING were reduced compared to the levels observed in WT mice following hepatic I/R injury (Fig. 2E). Moreover, IHC staining revealed that STING-KO mice had reduced p-TBK1 and p-P65 expression in I/R liver specimens compared with WT mice (Fig. 2F). Furthermore, STING-KO mouse liver specimens showed decreased proinflammatory cytokines/chemokines compared to those from WT controls (Fig. 2G). The findings indicate that the lack of STING protected liver damage and reduces the inflammatory reaction reduced by hepatic I/R injury.

Macrophages play a crucial role in the activation of the cGAS-STING signaling pathway during hepatic I/R injury

Given the importance of macrophage activation in hepatic I/R injury [22, 23] and the higher expression of STING in liver macrophages compared to hepatocytes [18, 24, 25], we questioned if liver macrophages play a major role in the activation of cGAS-STING pathway caused by liver ischemia-reperfusion injury. We extracted and purified mouse primary hepatocytes and primary liver macrophages from sham operation group or hepatic I/R model group, and found that the protein level of STING in liver macrophages is much higher than hepatocytes (Fig. S2A), and the upregulation of cGAS and STING in primary liver macrophages was significantly

more obvious than that in mPHs (Fig. S2B). Next, clodronate liposomes were used to scavenge macrophages by inducing apoptosis before ischemia (Fig. 3A). IHC staining and immunoblotting demonstrated that macrophages increases during liver ischemia-reperfusion injury (Fig. 3B, S2C). However, clodronate liposomes treatment resulted in the absence of macrophages, but not dendritic cells in liver tissues (Fig. S2C). The ALT and AST levels, H&E findings and TUNEL staining findings indicated that the removal of macrophages markedly reduce the liver damage caused by I/R (Fig. 3C-F).

As anticipated, the hepatic I/R injury led to a reduction in the cGAS-STING pathway when treated with clodronate liposomes (Fig. 3G-H). Figure 3I demonstrated that clodronate liposome treatment in hepatic I/R injury resulted in a decrease in the mRNA levels of liver proinflammatory cytokines/chemokines, as revealed by quantitative RT-PCR. Next, we reconstituted of macrophages to further suggest that the observed effect is macrophage dependent [26]. The results showed that the reconstructed macrophages group could reproduce the phenotype of control liposome group (Fig. 3J-L). These findings collectively indicate that eliminating macrophages can attenuate hepatic I/R damage and restrain the activation of the cGAS-STING signaling and inflammatory mediators.

Inhibitors of cGAS or STING protect against hepatic I/R injury

Given the notable increase of cGAS and STING in hepatic I/R injury and the protective effect of STING deletion against such injury, our subsequent objective was to confirm if the amelioration of hepatic I/R injury could be achieved by inhibiting either cGAS or STING. According to previous data, H151 exhibits significant inhibitory effects on STING in both humans and mice, demonstrating high potency and selectivity as a small-molecule antagonist [27]. G150, a potent small-molecule inhibitor of cGAS, exhibits inhibitory effects in both humans and mice [28]. The experimental procedures shown in Fig. 4A were followed to expose mice to these cGAS and STING inhibitors. After undergoing I/R surgery (Fig. 4B-C), the mice that received prior treatment with G150 or H151 exhibited decreased levels of ALT and AST activities. As anticipated, G150 or H151 effectively decreased the necrotic region and apoptosis during hepatic I/R injury, as shown in Fig. 4D-E. The findings indicate that inhibitors targeting cGAS or STING have a significant protective effect against hepatic I/R injury. Next, immune blot and IHC staining were used to show that compared with the control model group, p-TBK1 and p-p65 expression in the inhibitors of cGAS/STING treated groups was significantly reduced (Fig. 4F-G). Furthermore, the groups administered inhibitors exhibited

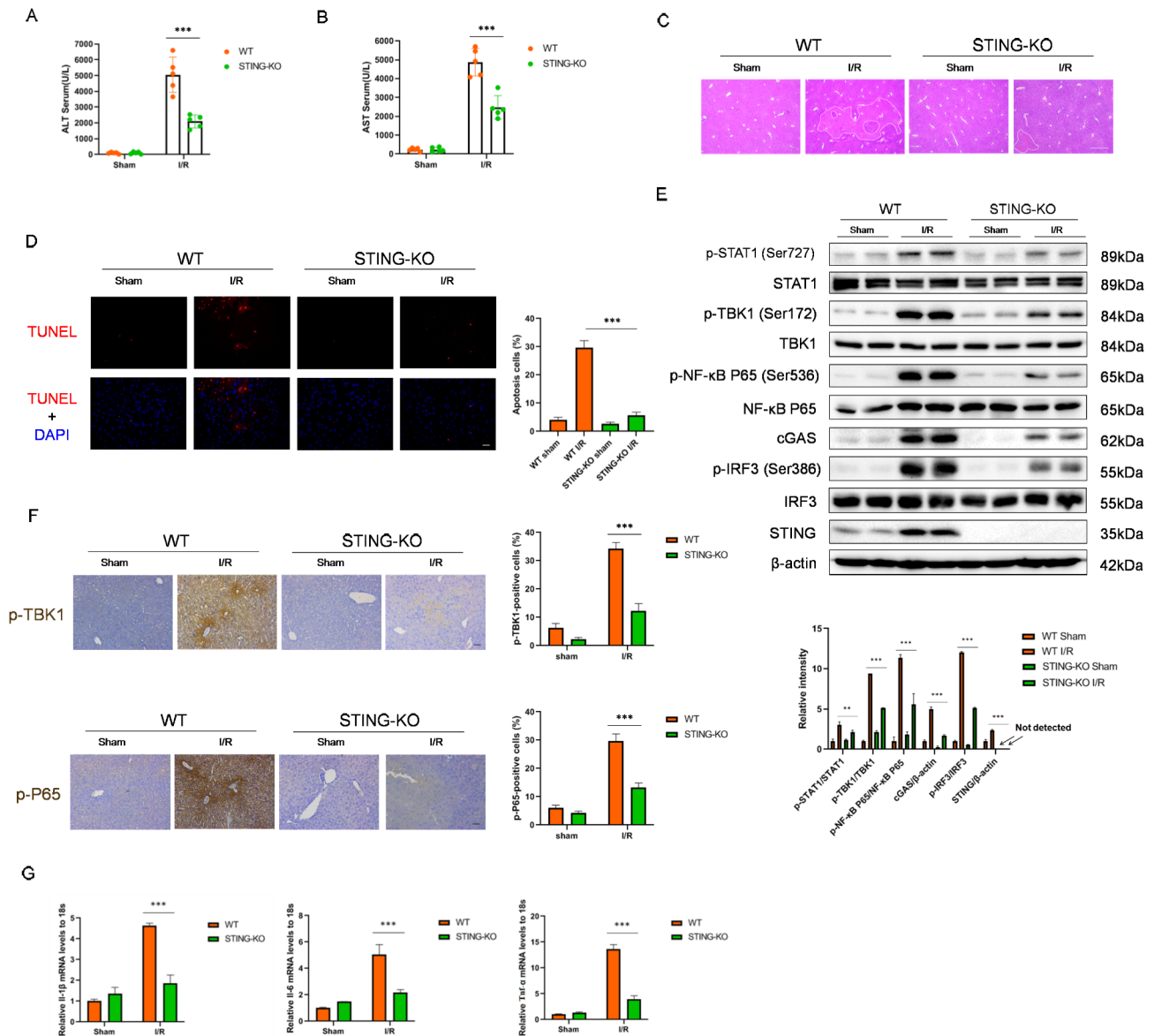


Fig. 2 STING deletion alleviates liver damage, inflammatory response and apoptosis during hepatic I/R injury. **(A–B)** Serum ALT/AST activities in WT and STING-KO mice at 6 h after hepatic I/R surgery ($n = 5$ per group). **(C)** Representative histological H&E-stained images of liver tissue from WT and STING-KO mice at 6 h after hepatic I/R surgery ($n = 3$ per group). Scale bar, 250 μm . **(D)** TUNEL staining in liver sections from WT and STING-KO mice at 6 h after hepatic I/R surgery ($n = 3$ per group). Scale bar, 25 μm . **(E)** Protein levels of the indicated genes in liver of WT and STING-KO mice at 6 h after hepatic I/R surgery. β -actin served as the loading control ($n = 2$ per group). **(F)** Representative IHC staining of p-TBK1 and p-P65 in liver tissue of WT and STING-KO mice at 6 h after hepatic I/R surgery ($n = 3$ per group). Scale bar, 50 μm . **(G)** mRNA levels of proinflammatory factors (IL1 β , IL6, and Tnf α) in liver tissue of WT and STING-KO mice at 6 h after hepatic I/R surgery. 18s served as the loading control. Levels of statistical significance are indicated as: * $p < 0.05$, ** $p < 0.01$, *** $p < 0.001$

a notable reduction in the mRNA levels of inflammatory factor, such as IL-6, TNF- α , and IL-1 β in liver tissues, as demonstrated by quantitative RT-PCR (Fig. 4J). The findings indicate that compounds targeting cGAS and STING can relieve I/R injury and inflammation in hepatic I/R injury.

The oxidative stress plays an important role in liver ischemia-reperfusion injury [29, 30], so we wanted to know if blocking the cGAS-STING pathway would affect ROS levels. We extracted and purified primary

hepatocytes from the sham group or hepatic I/R injury group with or without cGAS-STING inhibitors treatment, and detected the positive rate of ROS in the cells. After ischemia-reperfusion injury, ROS in hepatocytes was significantly up-regulated, but the inhibitors of cGAS-STING did not significantly affect the level of ROS (Fig. S3A–B). In addition, we extracted and purified primary hepatocytes to construct oxygen-glucose deprivation reperfusion (OGD-Rep) treatment models, with or without cGAS-STING inhibitors treatment. The results

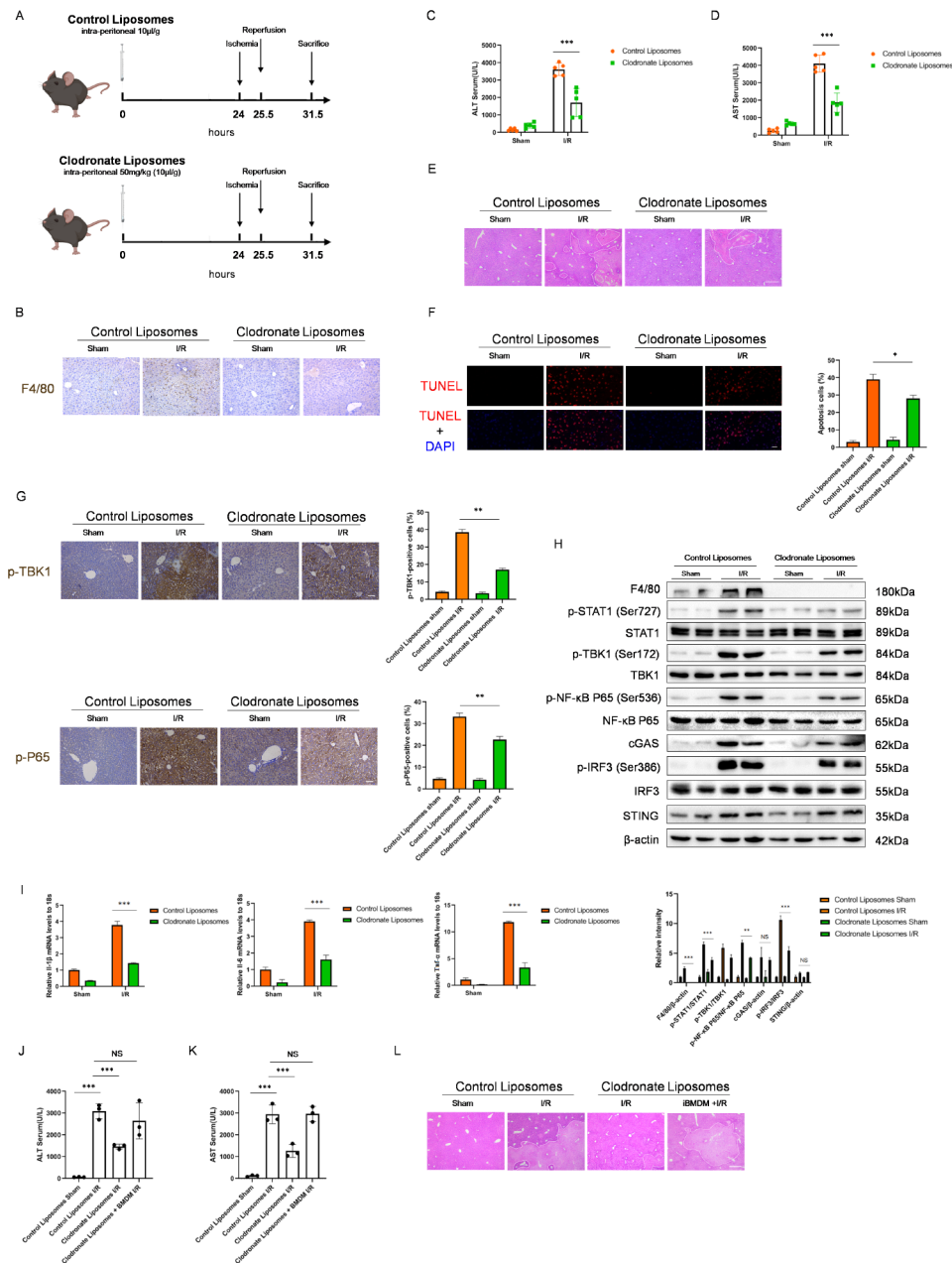


Fig. 3 Clearance of macrophages alleviates the activation of cGAS-STING pathway in hepatic I/R injury. **(A)** Schematic flowchart of sustained macrophages systemic scavenger by intermittent Clodronate Liposomes injection in vivo in the I/R mouse model. Clodronate Liposomes (50 µg/g) was intra-peritoneally injected into WT mice 24 h before ischemia. **(B)** IHC staining of F4/80 images of liver tissue from contrast and scavenger-treated mice at 6 h after hepatic I/R surgery ($n=3$ per group). Scale bar, 100 µm. **(C-D)** Serum ALT/AST activities in contrast and scavenger-treated mice at 6 h after hepatic I/R surgery ($n=5$ per group). **(E)** Representative histological H&E-stained images of liver tissue from contrast and scavenger-treated mice at 6 h after hepatic I/R surgery ($n=3$ per group). Scale bar, 250 µm. **(F)** TUNEL staining in liver sections from contrast and scavenger-treated mice at 6 h after hepatic I/R surgery ($n=3$ per group). Scale bar, 25 µm. **(G)** Protein levels of the cGAS-STING pathway molecules in liver of contrast and scavenger-treated at 6 h after hepatic I/R surgery. β -actin served as the loading control ($n=2$ per group). **(H)** Representative p-TBK1 and p-P65 IHC staining in liver tissue of contrast and scavenger-treated mice at 6 h after hepatic I/R surgery ($n=3$ per group). Scale bar, 50 µm. **(I)** mRNA levels of proinflammatory factors (IL1 β , IL6, and Tnfa) in liver tissue of contrast and scavenger-treated mice at 6 h after hepatic I/R surgery. 18s served as the loading control. **(J-K)** Serum ALT/AST activities in contrast, scavenger-treated and macrophage-reconstituted mice at 6 h after hepatic I/R surgery ($n=3$ per group). **(L)** Representative histological H&E-stained images of liver tissue from contrast, scavenger-treated and macrophage-reconstituted mice at 6 h after hepatic I/R surgery ($n=3$ per group). Scale bar, 250 µm. Levels of statistical significance are indicated as: * $p < 0.05$, ** $p < 0.01$, *** $p < 0.001$

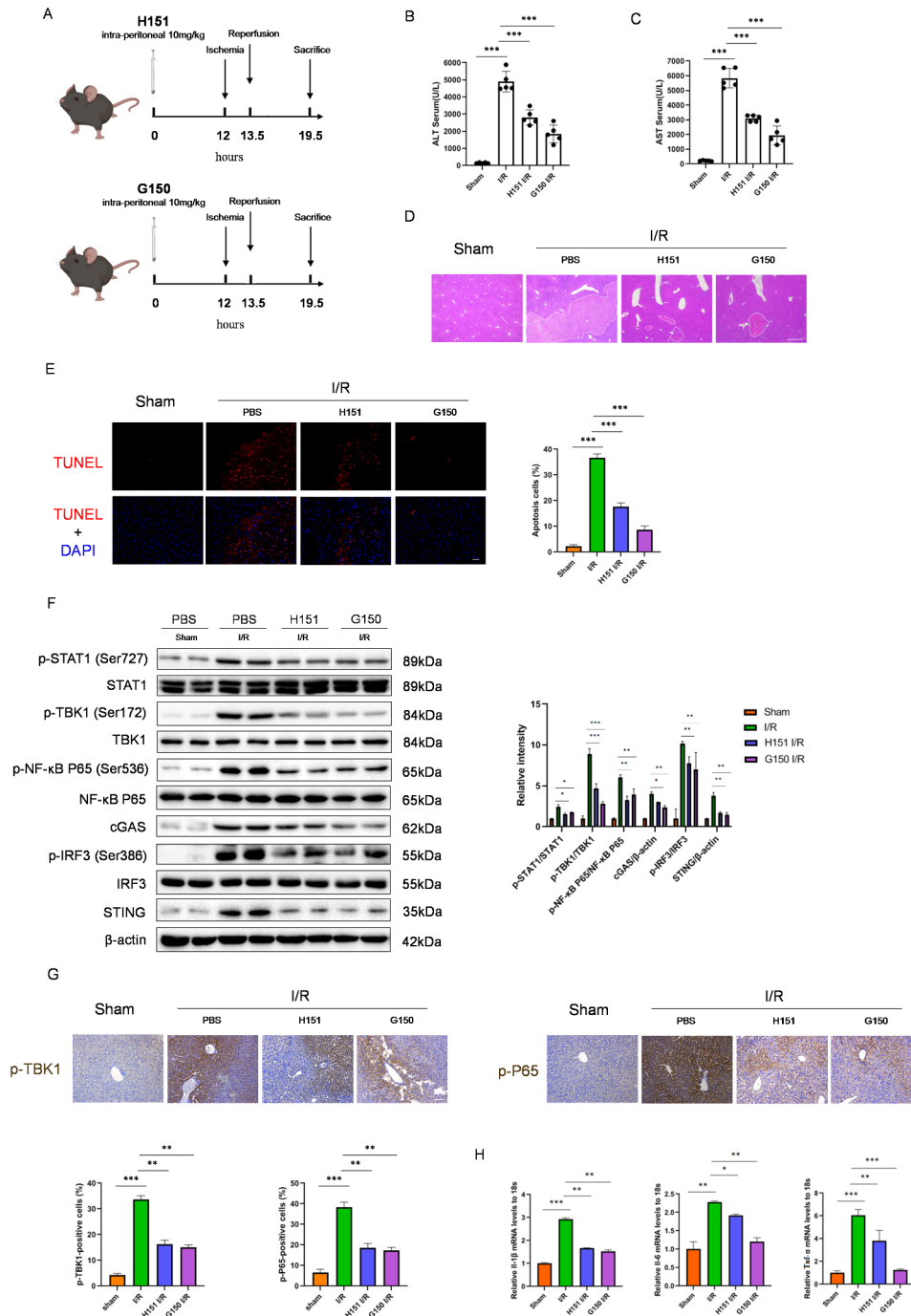


Fig. 4 The blockade of STING and cGAS promotes liver protection during hepatic I/R injury. **(A)** Schematic flowchart of sustained STING and cGAS blockade by intermittent H151 and G150 injection in vivo in the I/R mouse model separately. H151 (10 μg/g) or G150 (10 μg/g) was intraperitoneally injected into WT mice 12 h before ischemia. **(B–C)** Serum ALT/AST activities in contrast and inhibitor-treated mice at 6 h after hepatic I/R surgery ($n = 5$ per group). **(D)** Representative histological H&E-stained images of liver tissue from contrast and inhibitor-treated mice at 6 h after hepatic I/R surgery ($n = 3$ per group). Scale bar, 250 μm. **(E)** TUNEL staining in liver sections from contrast and inhibitor-treated mice at 6 h after hepatic I/R surgery ($n = 3$ per group). Scale bar, 25 μm. **(F)** Protein levels of the cGAS-STING pathway molecules in liver of contrast and inhibitors-treated at 6 h after hepatic I/R surgery. β-actin served as the loading control ($n = 2$ per group). **(G)** Representative p-TBK1 and p-P65 IHC staining in liver tissue of contrast and inhibitor-treated mice at 6 h after hepatic I/R surgery ($n = 3$ per group). Scale bar, 50 μm. **(H)** mRNA levels of proinflammatory factors (Il1β, Il6, and Tnfa) in liver tissue of contrast and inhibitor-treated mice at 6 h after hepatic I/R surgery. 18s served as the loading control. Levels of statistical significance are indicated as: * $p < 0.05$, ** $p < 0.01$, *** $p < 0.001$

reached a consistent conclusion (Fig. S3C-D). The above results indicate that hepatic I/R injury can lead to the upregulation of ROS in hepatocytes, but inhibition of cGAS-STING does not affect the changes of ROS.

Blocking release of mtDNA alleviates hepatic I/R injury

It is well known that DNA is the most important ligand that activates the cGAS-STING pathway. Furthermore, we observed a notable increase in serum DNA levels during hepatic I/R injury (Fig. S4A), leading us to hypothesize that DNA is responsible for triggering the activation of the cGAS-STING signaling pathway. The DNA of a cell is mainly contained in the nucleus and mitochondria, and we found that mtDNA increased significantly after hepatic I/R injury compared to nuclear DNA (Fig. S4B-C). Moreover, we performed immunofluorescence confocal staining of DNA in frozen sections of mouse liver tissue of sham operation group or the hepatic I/R model group. The results showed that in the sham group, the extranuclear DNA had significant colocalization with the mitochondria, but in the hepatic I/R model group, the extranuclear DNA was located outside the mitochondria (Fig. S4D). It has been reported that TFAM could be released concurrently with mtDNA [31, 32], and our results suggest that TFAM is also released in serum in hepatic I/R injury (Fig. S4E). These results suggest that mtDNA is released from mitochondria after liver ischemia-reperfusion injury. Next, we want to study which cells these mtDNAs come from. Previous reports have suggested that hepatocyte injury and macrophage inflammation are the main adverse factors in liver ischemia-reperfusion injury [33–36]. We specifically extracted hepatocytes and macrophages to construct OGD-rep treatment models to detect the release of mtDNA, and found hepatocytes had significantly more mtDNA release (Fig. S4F-I). These results suggest that the mtDNA release in liver ischemia-reperfusion injury is mainly derived from hepatocytes.

According to previous reports, mtDNA fragments are known to leave mitochondria through mPTP and VDAC channels [37]. Then, we tried to use CsA (an mPTP inhibitor) and VBIT4 (a VDAC inhibitor) to block the release of mtDNA. According to reports, the release of cytoplasmic mtDNA was increased following the administration of ABT737 (an inhibitor of Bcl2) and Z-VAD-FMK (an inhibitor of caspases) [38, 39]. When we treated the cells with CsA and VBIT, we found that mtDNA was indeed significantly downregulated (Fig. S5A). Furthermore, the activation of the cGAS-STING pathway caused by the release of mtDNA was considerably suppressed (Fig. S5B-C).

Subsequently, we assessed the therapeutic capacity of these blockers in hepatic I/R damage. The experimental procedures shown in Fig. 5A were followed to expose

mice to either mPTP or VDAC inhibitors. In hepatic I/R injury, the release of mtDNA in serum was significantly reduced by these inhibitors according to quantitative RT-PCR experiments. However, the content of nuclear DNA remained unaffected (Fig. 5B-C). ALT and AST levels were also significantly attenuated in the inhibitor pretreatment groups (Fig. 5D-E). In accordance with these findings, CsA- or VBIT4-treated mice exhibited decreased necrotic areas and apoptosis, as demonstrated by H&E analysis and TUNEL staining (Fig. 5F-G). As expected, CsA and VBIT4 also inhibited cGAS and STING expression, cGAS-STING activation and inflammatory factors (Fig. 5H-J).

The current studies shows that Bax/Bak is mainly responsible for punching holes in the outer membrane (OMM) of mitochondria and promoting the release of mitochondrial contents [40]. To investigate whether Bax/Bak also affects liver ischemia-reperfusion injury through regulating the release of mtDNA, we have treated mice with Bax/Bak inhibitor (MSN-125) and found that the release of mtDNA was downregulated, and cGAS/STING activation and inflammation induced by hepatic I/R injury was also significantly inhibited (Fig. S6A-D). These findings collectively indicate that suppressing the release of mtDNA can relieve hepatic I/R injury by obstructing the cGAS-STING signaling pathway.

Safety assessment of inhibitors at the animal level

Given that inhibitors of cGAS, STING, and mtDNA channels have the ability to provide substantial protection against hepatic I/R injury, it is plausible that these inhibitors could be utilized as promising pharmaceuticals for the management of hepatic I/R injury. Therefore, we next evaluated whether the inhibitors caused harm to important tissues. We conducted a new batch of animal experiments using the previous dosage and administration method of these inhibitors. The serum biochemical parameters of the mice in each group, such as ALT, AST, blood urea nitrogen, and creatinine, were all within the normal ranges as shown in Fig. 6A and C. Additionally, the histological evaluations revealed the absence of any histopathological abnormalities in the primary organs of mice that underwent treatment with the inhibitor (Fig. 6B, D). These results confirmed that treatment with these inhibitors is not toxic to mice.

Discussion

Hepatic I/R injury is a complex disease regulated by multiple signaling pathways with the involvement of multiple cells in the liver. In this paper, we reveal the role of activation of cGAS-STING signaling pathway in the process of hepatic I/R injury from the perspective of innate immunity, and describe how cGAS-STING pathway is activated and involved in hepatic I/R injury. Our finding

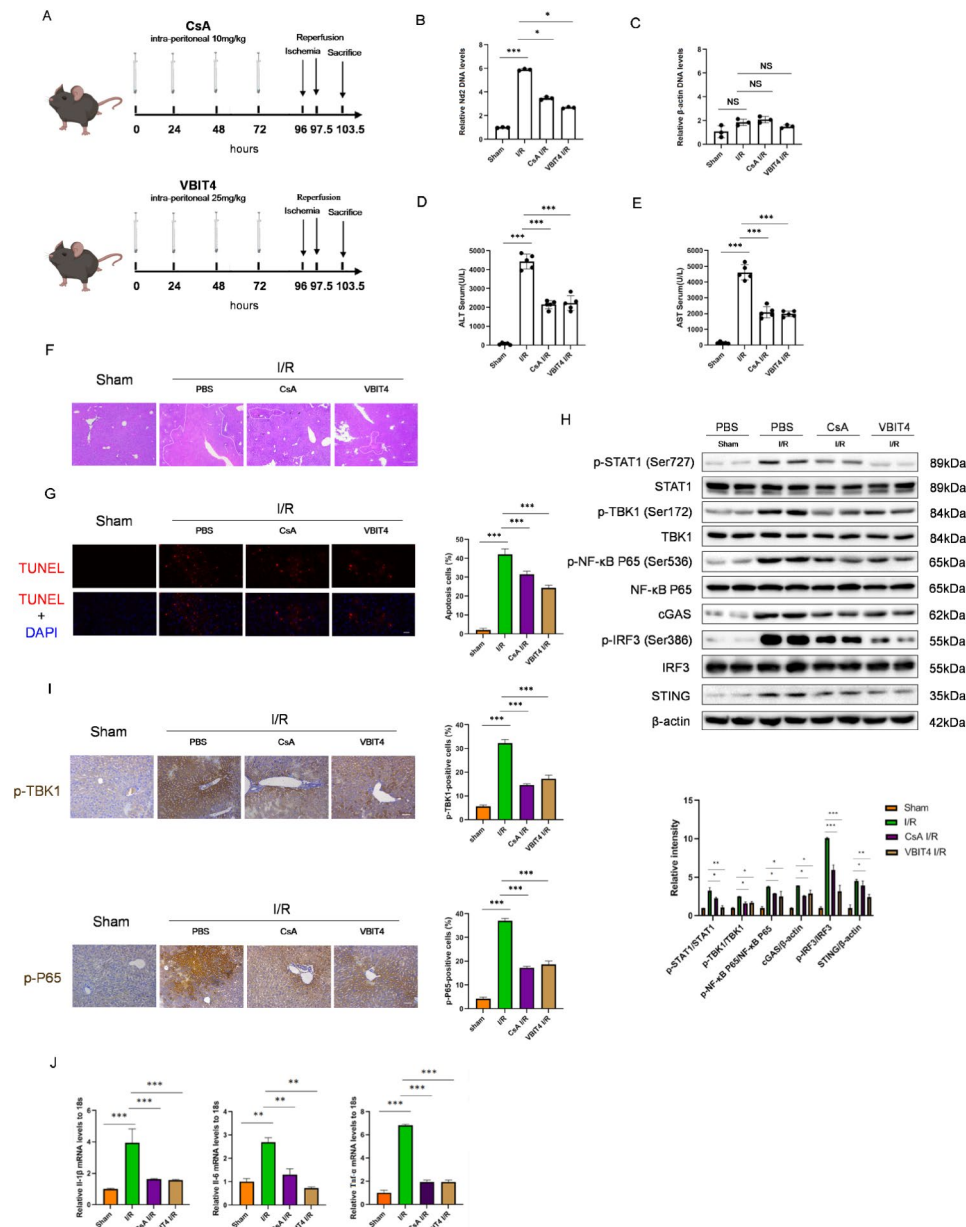


Fig. 5 Preventing mtDNA escape promotes liver protection during hepatic I/R injury. **(A)** Schematic flowchart of sustained mPTP and VDAC channels inhibition by intermittent CsA and VBIT4 injection in vivo in the I/R mouse model separately. CsA (10 µg/g) or VBIT4 (25 µg/g) was intraperitoneally injected into WT mice 96, 72, 48 and 24 h before ischemia. **(B–C)** Relative mitochondrial and nuclear DNA levels detected in serum of WT mice with or without mtDNA release inhibitor at 6 h after hepatic I/R surgery ($n=3$). Mitochondrial DNA present in mouse serum samples was assessed by qPCR using ND2. Nuclear DNA was amplified using β-actin. **(D–E)** Serum ALT/AST activities in contrast and mtDNA-escaping-inhibitor-treated mice at 6 h after hepatic I/R surgery ($n=5$ per group). **(F)** Representative histological H&E-stained images of liver tissue from contrast and mtDNA-escaping-inhibitor-treated mice at 6 h after hepatic I/R surgery ($n=3$ per group). Scale bar, 250 µm. **(G)** TUNEL staining in liver sections from contrast and mtDNA-escaping-inhibitor-treated mice at 6 h after hepatic I/R surgery ($n=3$ per group). Scale bar, 25 µm. **(H)** Protein levels of the cGAS-STING pathway molecules in liver of contrast and mtDNA-escaping-inhibitor-treated at 6 h after hepatic I/R surgery. β-actin served as the loading control ($n=2$ per group). **(I)** Representative p-TBK1 and p-P65 IHC staining in liver tissue of contrast and mtDNA-escaping-inhibitor-treated mice at 6 h after hepatic I/R surgery ($n=3$ per group). Scale bar, 50 µm. **(J)** mRNA levels of proinflammatory factors (Il1β, Il6, and Tnfa) in liver tissue of contrast and mtDNA-escaping-inhibitor-treated mice at 6 h after hepatic I/R surgery. 18s served as the loading control. Levels of statistical significance are indicated as: * $p<0.05$, ** $p<0.01$, *** $p<0.001$

indicates that mice lacking STING can prevent liver I/R damage. Furthermore, the cGAS-STING signaling pathway plays a crucial role in controlling hepatic I/R injury, and directing attention towards this pathway could be a

hopeful strategy to safeguard the liver from I/R-induced harm in individuals receiving transplants. During hepatic I/R injury, liver cells suffer damage and even die, and then the released mitochondrial DNA from damage liver cells

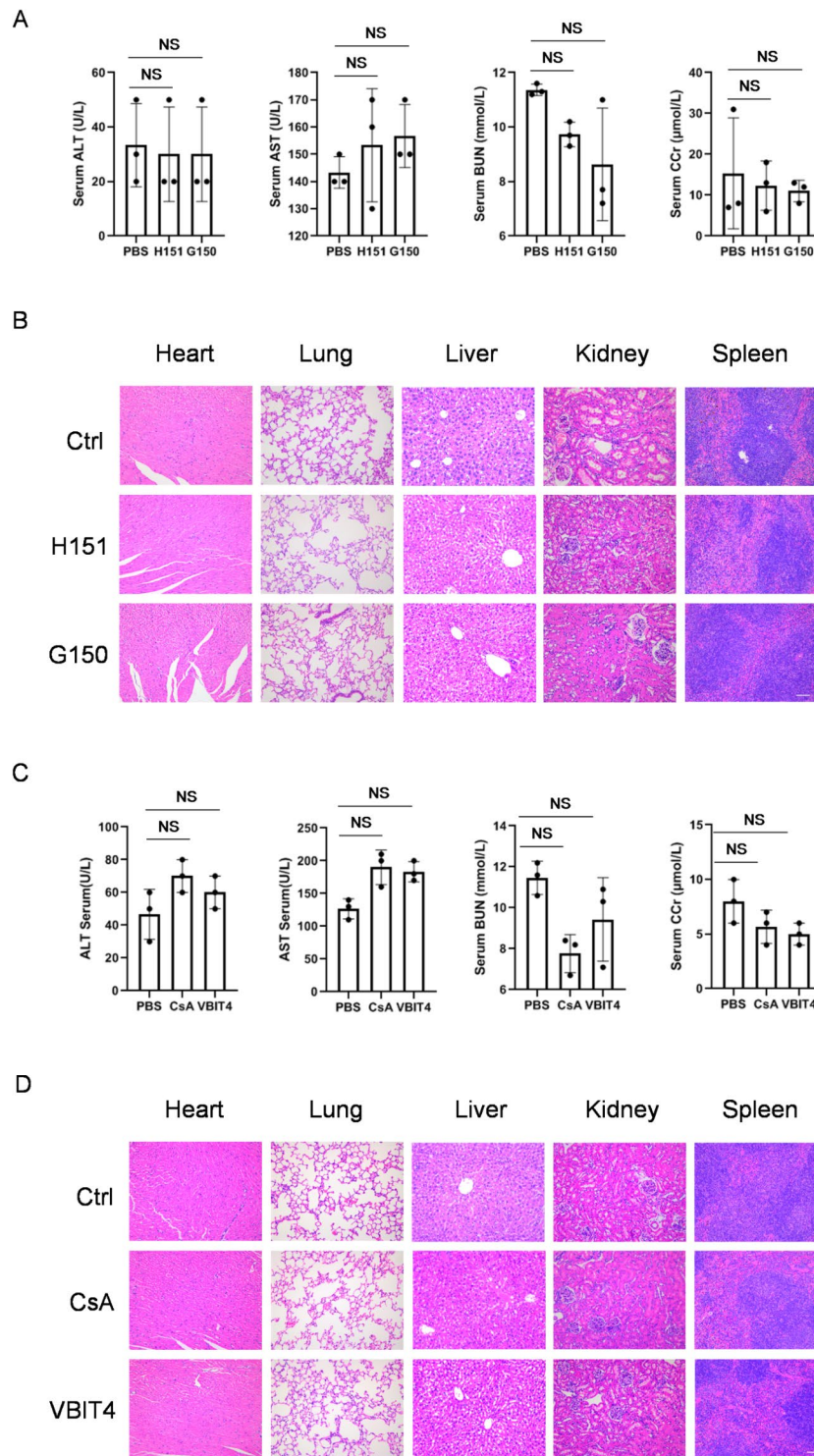


Fig. 6 Safety evaluation of inhibitors (H151, G150, CsA and VBIT4) of cGAS-STING pathway in mice. **(A-C)** Serum levels of alanine transaminase (ALT), aspartate aminotransferase (AST), blood urea nitrogen (BUN), and creatinine (Cr) in mice were measured 24 h after intraperitoneally injected. **(B-D)** H&E staining for heart, lung, liver, kidney and spleen from mice in each group. Scale bar, 100 μm. Levels of statistical significance are indicated as: * $p < 0.05$, ** $p < 0.01$, *** $p < 0.001$

were recognized by some kinds of cells of liver, especially macrophages. Inflammation initiated by cGAS-STING further aggravates hepatic I/R injury. Inhibition of mtDNA release or inhibitors of cGAS-STING activity can significantly improve liver damage (Fig. 7).

The process of liver I/R injury is a complicated pathophysiological phenomenon that includes multiple signaling pathways. Due to the global scarcity of donated organs, liver transplantations often utilize expanded criteria donor (ECD) organs, which include organs from older individuals, those with fatty liver, and donors who experienced cardiac arrest and/or brain death. This practice significantly increases the likelihood of hepatic I/R injury [41]. Our findings in this research suggest that hepatic I/R damage poses a significant barrier to increasing the availability of donor organs for liver transplant procedures. Extensive research has been conducted in the past ten years to investigate the pathophysiology of hepatic I/R injury and discover specific treatments to mitigate its adverse effects [9]. The treatment of acute complications with effective drugs is beneficial. Numerous medications have undergone testing in order to prevent and treat hepatic I/R injury, which encompasses various activators and inhibitors of signaling pathways. Promising treatment strategies, including Akt stimulators, AMPK stimulators, and PPAR γ agonists, have been identified and require additional clinical investigation [9, 42–44]. Nevertheless, liver surgery still faces the challenge of unresolved hepatic I/R injury, possibly due to the limited translation of basic research discoveries into

clinical practice. Additional research is required to seek valuable solutions.

Hepatic ischemia/reperfusion (I/R) damage involves aseptic inflammation controlled by the innate immune cells of liver were activated by the PRRs encoded by DAMPs. Induced stress triggers the activation of macrophages, leading to the production of ROS [46]. These ROS then cause oxidative damage to the mitochondria, initiating in the release of mtDNA into the cytosol [47]. The amount of mtDNA released from liver cells is significantly higher during hepatic ischemia/reperfusion injury [48]. The mtDNA released mainly from damaging hepatocytes and inner damaged mitochondria is a crucial DAMP. The cGAS, a well-documented PRR, can effectively interact with mtDNA, resulting in the activation of signaling pathways through catalyzes the synthesis of cyclic GMP-AMP (cGAMP). Subsequently, STING, the downstream effector protein, is recruited by cGAMP [49]. The cGAMP attached to STING promoted the movement of STING from the endoplasmic reticulum to the Golgi apparatus and triggered the activation of TBK1 [50]. TBK1 phosphorylates different transcription factors, including NF- κ B and IRF3, promotes the transcription of specific inflammatory cytokines, such as IL1 β , IL18, IL6, and TNF- α , and IFN-stimulating genes [51, 52]. In this study, we demonstrated that inhibition of cGAS-STING can effectively alleviate liver I/R injury through a series of experiments including STING knockout mice, cGAS-STING inhibitors, and macrophage scavenger, and the release of mtDNA is the main

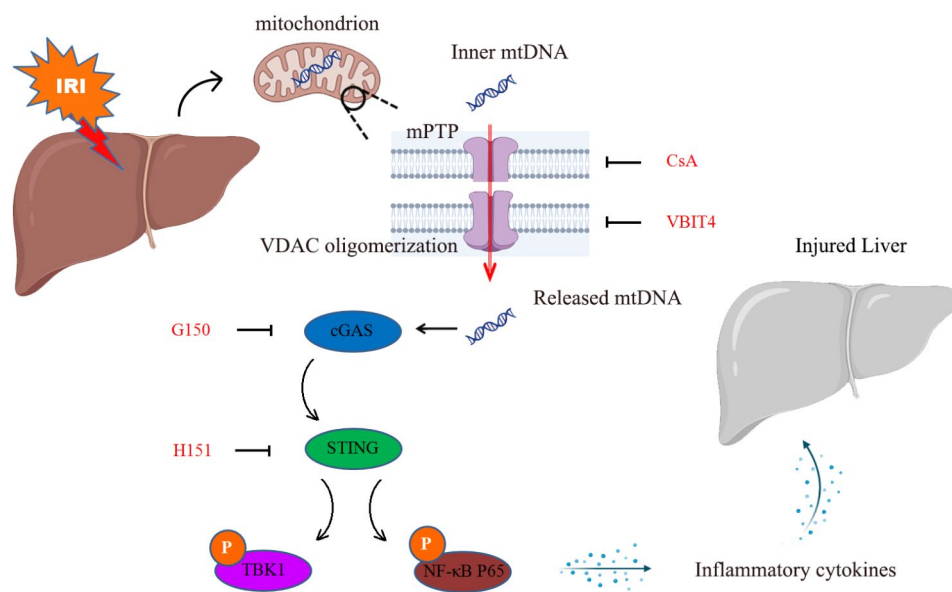


Fig. 7 Schematic model of targeting cGAS-STING to regulate hepatic ischemia-reperfusion. The mtDNA was released in hepatic I/R injury, then triggered the activation of cGAS-STING signaling pathway. The inflammatory cytokines induced by cGAS-STING pathway aggravated liver damage. Small molecule inhibitors like CsA, VBIT4, H151 and G150 can inhibit the release of mtDNA or activation of cGAS-STING signaling significantly reduced liver damage

factor of cGAS-STING activation. Considering that there are other DNA recognition receptors in the cell, such as AIM2, IFIT1, etc., these receptors can also activate the inflammatory response. Therefore, in this paper, we used to inhibit the release of mtDNA to inhibit the mtDNA-induced inflammatory response.

Recent studies have provided compelling evidence for the crucial role of the mtDNA-cGAS-STING pathway, particularly in liver macrophages, in hepatic I/R injury. While an initial research suggested no connection between hepatic I/R injury and activation of the cGAS-STING signaling pathway, it did find that cGAS regulates autophagy in hepatocytes independently of STING to safeguard the liver [53]. In a mouse model [54], MicroRNA-24-3p has the ability to decrease STING signaling and diminish the levels of p-TBK1, p-IRF3, and transferase in hepatic I/R injury. Stimulation of I/R and mtDNA can boost the protein amounts of p-STING and p-TBK1 in the KCs of elderly mice, leading to elevated production of proinflammatory cytokines/chemokines by macrophages, ultimately worsening hepatic I/R injury [55]. In liver macrophages, the suppression of STING decreases hepatic I/R injury mediated by macrophage caspase 1-GSDMD and dependent on calcium signaling [22]. Hepatic I/R stress triggers inflammation and cell death through the CYLD-NRF2-OASL1 pathway, which regulates STING-TBK1-dependent apoptotic/necrotic responses [23]. These findings suggest that focusing on mtDNA-cGAS-STING signaling pathway could be a crucial approach for managing hepatic I/R injury.

Consistent with the aforementioned studies [22, 23, 55], our loss-of-function experiments involving STING provided confirmation of its role in regulating inflammation in hepatic I/R injury. The symptoms observed in STING-KO mice were replicated by H151, a pharmacological inhibitor of STING, suggesting its potential use in patients experiencing hepatic I/R injury. Upstream factors regulate the substantial increase in STING expression during hepatic I/R injury. We then studied the inhibitors of cGAS/STING and the mtDNA-escaping inhibitors CsA and VBIT4 and obtained similar results. The results indicate that strategies aimed at inhibiting cGAS-STING and/or preventing mtDNA escape could be effective in treating hepatic I/R injuries. Several related drugs inhibiting the mtDNA-cGAS-STING pathway have been approved for clinical application. These results may lead to expanded clinical use of drugs that inhibit mtDNA release, as well as inhibitors of the cGAS-STING pathway to the benefit of patients.

During hepatic I/R injury, liver macrophages, consisting of resident KCs and infiltrated macrophages derived from bone marrow (BMDMs), actively participate in innate immune responses. Previous studies focused on mtDNA-cGAS-STING pathway activation in liver

macrophages [22, 23]. Interestingly, when liver macrophages were scavenged by clodronate liposomes, the mtDNA-cGAS-STING pathway could still be activated widely in I/R liver tissues in our study. According to a recent investigation, the activation of STING signaling in liver cells is only marginally increased during hepatic I/R injury [55]. The implications of these findings suggest that liver innate immune cells, especially macrophages, are activated by mtDNA released by liver cells to promote liver I/R damage through the cGAS-STING pathway, ultimately leading to a cascade of liver damage.

The mouse model of hepatic I/R injury, which is known for its 70% warmth, is widely accepted in I/R studies; however, it is undeniably a stringent model. Every case in the clinic is different, which means that primary animal model research is still far from clinical application. We need more statistics to support these results and further studies to push them to clinical application. In this study, we evaluated two inhibitors of cGAS-STING and two small molecule drugs that inhibit mtDNA release and found that they are not significantly toxic, but have a good protective effect in liver I/R injury. We believe that the four small molecule compounds can be further tested by clinical trials to evaluate the efficacy and safety of treatment in patients suffering from hepatic I/R injury. If the clinical trials can be successful, more options for treatment of hepatic I/R injury could be provided. Although cGAS-STING inhibitors have been shown to alleviate liver I/R injury well, mtDNA can also damage the liver through other DNA receptors, so inhibiting the release of mtDNA may be more advantageous in the treatment of liver I/R injury diseases. Consider that there are currently no inhibitors of cGAS-STING approved for clinical use, while mtDNA inhibitors, such as CsA, is a small molecule drug approved by FDA, which means it has a greater hope of being applied to clinical treatment as soon as possible.

Materials and methods

Reagents

The STING antagonist H151 (10 mg/kg, S6652) was purchased from Selleckchem. MedChemExpress was the source of the purchased cGAS inhibitor G150 (10 mg/kg, HY-128583), mPTP inhibitor Cyclosporin A (CsA, 10 mg/kg, HY-B0579) and Bax/Bak inhibitor MSN-125 (5 mg/kg, HY-120079). Aladdin sold the VBIT4 (25 mg/kg, 2086257-77-2), an inhibitor of VDAC oligomerization. Yeasen sold the macrophage scavenger clodronate and control liposomes (50 mg/kg, 40337ES; 10 µl/g, 40338ES).

Clinical samples

Recruitment took place at the Third Affiliated Hospital of Sun Yat-Sen University (Guangzhou, China), involving

a total of five individuals who had undergone liver transplants.

Cell culture and animals

The Hep3B cell line was purchased from ATCC, which were grown in DMEM (Gibco) containing 10% FBS (PAN-B iotech) at a temperature of 37 °C with 5% CO₂. C57BL/6 male mice, aged 8–10 weeks, are acquired from Bestest Biotechnology located in ZhuHai, Guangdong. STING knockout mice were obtained from the Jackson Laboratory. Every mouse was bred in a controlled environment free from any pathogens. The Ethics Committee approved all procedures involving animals.

Mouse hepatic I/R injury model establishment

As previously documented [56], we employed a commonly used mouse liver I/R injury model, which involved warming the mice to 70% of their normal body temperature. Typically, the mice were sedated using 1% pentobarbital, and a surgical incision was made along the midline to reveal the liver. Then, an atraumatic microvascular clamp was used to clamp the branches of the left and middle portal veins in the liver, effectively interrupting the blood supply. Following a 90-minute period of ischemia, the clamp was subsequently removed to allow for reperfusion. Following a 6-hour reperfusion period, the mice were once again anesthetized using 1% pentobarbital in order to obtain serum and liver samples for subsequent analysis. Sham controls were used as a comparison group for mice that underwent a surgical procedure without occlusion of blood vessels. Data from every mouse that died before sample collection were discarded. A single operator conducted all procedures, and the mice underwent a 12-hour fasting period prior to the surgery.

Isolation of primary hepatocytes and liver macrophages

Primary hepatocytes and liver macrophages from WT mice were isolated as reported [57].

Histological staining

Formalin was used to fix liver samples, which were then embedded in paraffin and serially sectioned at a thickness of 4 to 5 micrometers. Following the removal of paraffin and restoration of moisture, a conventional staining technique using H&E was performed to observe the arrangement in areas of liver necrosis. The light microscope (Leica DFC310 FX, Wetzlar, German) was utilized to observe and capture images.

Immunohistochemistry, immunofluorescence and TUNEL staining

The sections were treated with xylene to remove the wax, and then washed using a series of ethyl alcohol solutions. Next, these sections underwent antigen-repairing with

a solution of citrate buffer and heated for a duration for 25 min. Afterward, the sections were treated with H₂O₂ at a temperature of 37 °C for 10 min. Following this, the sections were exposed to primary antibodies against cGAS (1:100, #15102 and 1:100, #31659, CST), STING (1:25, #13647, CST), phospho-TBK1 (Ser172) (1:50, #5483, CST), phospho-NF-κB P65 (Ser536) (1:50, #3033, CST), and F4/80 (1:100, #70076, CST) overnight at a temperature of 4 °C. Finally, these sections were incubated using indicated secondary antibodies for a period of 30 min at a temperature of 37 °C. For immunofluorescence, the sections were treated with self-fluorescence quenching kit (Cat: #G1221; Servicebio) after antigen-repairing. Then, the sections were exposed to primary antibodies both mouse anti-DNA (1:50, #4093091, Millipore) and rabbit anti-Tomm20 (1:50, #11802-1, Proteintech) overnight at a temperature of 4 °C. Finally, these sections were incubated using indicated a mixture of Alexa Fluor™ 594 donkey anti-Mouse IgG (1:500, A-21203, Lifetechnologies) and Alexa Fluor™ 488 donkey anti-Rabbit IgG (1:500, A-21206, Lifetechnologies) for a period of 60 min at a temperature of 37 °C. Apoptosis in the liver was detected using TUNEL staining, following the manufacturer's protocol (Servicebio, 1689925873930ZKTtPJ). Next, the sections were treated with a staining solution consisting of DAB, H₂O₂, and PBS for visualization. Afterwards, the segments were treated with hematoxylin for a duration of 30 s under normal room temperature. In the end, the sections were stripped of wax using xylene and washed with a varying concentration of ethyl alcohol. Using an inverted microscope, the observation of the staining was made for each section. Image J software was used for quantification analysis of IHC.

Quantitative RT-PCR

ChamQ SYBR qPCR Master Mix (Catalog No. was used for conducting quantitative RT-PCR analyses. The quantification of mRNA expression was performed at Vazme in Nanjing, China, following the described methods. The results of qPCR were normalized according to 18 S expression. The sequences of primer were as stated below.

18 S forward, GTAACCCGTTGAACCCCAT; 18 S reverse, CCATCCAATCGGTAGTAGCG;

Sting forward, TAGAGAGCTTTGGGGCCTCT; Sting reverse, TGGAGTATGGCATCAGCAGC;

cGas forward, GCTCACAAAGATGCACAGC; cGas reverse, GGTCCCCTTACGACTTTCCG;

Tbk1 forward, ATCAAGAAGGCACGCATCCA, Tbk1 reverse, GGCTCATTGCTTTTGTGGCA;

P65 forward, CATCGCAGGACAAGACCTCA, P65 reverse, ACCTTCTGTCCACCTCCGAT;

Irf3 forward: AGCCCTGAACCGGAAAGAAG; Irf3 reverse: CCCAGATGTACGAAGTCCCG;

IL-1 β forward, TGAAATGCCACCTTTTGACAGTG;
IL-1 β reverse, ATGTGCTGCTGCGAGATTTG;

IL-6 forward, TGATGGATGCTACCAAAGTGA; IL-6
reverse, TGTGACTCCAGCTTATCTCTTG;

Tnf- α forward, GATCGGTCCCCAAAGGGATG;
Tnf- α reverse, TTTGCTACGACGTGGGCTAC;

Nd2 forward, CCCATTCCACTTCTGATTACC; Nd2
reverse, ATGATAGTAGAGTTGA GTAGCG;

β -actin forward, GATATCGCTGCGCTGGTTCG;
 β -actin reverse, CATTCCCACCATCACACCCT;

ND1 forward: CCCTAAAACCCGCCACATCT; ND1
reverse: GAGCGATGGTGAGAGCTAAGGT;

IL-1 β forward, CTGAGCTCGCCAGTGAAATG;
IL-1 β reverse, CCCTTGCTGTAGTGGTGGTC;

IL-6 forward, AACTCCTTCTCCACAAGCGCC, IL-6
reverse, TTGGAATCTTCTCCTGGGGGTA;

TNF- α forward, GCTGCACTTTGGAGTGATCG;
TNF- α reverse, TCACTCGGGGTTTCGAGAAGA.

Expression level of released DNA detection

The released DNA in mouse serum and supernatant of cells were detected and quantified as previously described [58]. In detail, isolated mouse serum (100 μ l) or cell supernatant (200 μ l) was further filtrated with a 0.2 μ m PES membrane (Sartorius VS0171). DNA was isolated from the ultra-filtrated fluid using the QiAmp DNA extraction kit (Qiagen, 51306) following manufacturer's recommendations. Mitochondrial DNA present in the samples was assessed by qPCR using ND1, while ND2 was used for the murine derived samples. Nuclear DNA present in samples was assessed by qRT-PCR using β -actin.

Immunoblotting

Protein levels were evaluated using immunoblotting analysis, as reported. Signals of immune blot were detected using a Tanon 5200 ChemiDoc MP Imaging System. The quantification of protein levels was performed using ImageJ software. All antibodies of immune blot were as stated below:

Anti-F4/80 (1:1,000, #70076), anti-pTBK1 (1:1,000, #5483), anti-TBK1 (1:1,000, #38066), anti-p-p65 (1:1,000, #3033), anti-cGAS (1:1,000, #15102 and 1:1,000, #31659), anti-STING (1:1,000, #13647), anti-CD11c (1:1,000, #97585) and anti- α -tubulin (1:5,000, #2125) were purchased from Cell Signaling Technology. HuaBio offers anti-phospho-STAT1 (1:1,000, HP0221), anti-p65 (1:1,000, HP0221), anti- β -actin (1:4,000, HA601037), and anti-IRF3 (1:2,000, HO0118) antibodies. Anti-STAT1 (1:2,000, #00077121) was from Proteintech, anti-p-IRF3 (1:1,000, ab76493) was from Abcam; Secondary antibodies (1:3,000, #7074, 1:3,000, #7076) were from Cell Signaling Technology.

Flow cytometry

ROS was tested using MitoSOX Red staining (Cat: #HY-D1055; MCE) according to the manufacturer's protocol.

ELISA assays

TFAM was detected using an enzyme-linked immunosorbent assay kit (Cat: #24080; Jiangsu Meimian Industrial Co., Ltd).

Statistical analysis

The SPSS software (18.0) was utilized all statistical analyses. The results are presented as the mean \pm SEM. The Student's t test and a one-way ANOVA was used to compare multiple groups. A significance level of less than 0.05 was deemed statistically significant.

Supplementary Information

The online version contains supplementary material available at <https://doi.org/10.1186/s12967-024-05588-8>.

Supplementary Material 1

Supplementary Material 2

Supplementary Material 3

Supplementary Material 4

Supplementary Material 5

Supplementary Material 6

Supplementary Material 7

Acknowledgements

Not applicable.

Author contributions

QZ, YQ and DQ studied concept and designed the study; YX, JC, WL, YH and JS conducted experiments; KL acquired patient specimens; YX, KL, YH and JS acquired, analyzed and interpreted data; YX, JC and WL drafted the manuscript; BZ and XQ offered project administration and resources; DQ, QZ and YQ made critical revision of the manuscript.

Funding

The National Natural Science Foundation of China (81970509, 81800559), the Natural Science Foundation of Guangdong Province (2022A1515012223, 2023A1515011615), the Science and Technology Program of Guangzhou, China (202201020430, 2023A03J0195, 2023A04J1797), and the Basic Research Funds for the Central Universities (23ykj005) provided funding for this project.

Data availability

Data sets used during this study were available from the corresponding authors.

Declarations

Ethics approval and consent to participate

This study was reviewed and approved by the Ethics Committee (ethics approval number: RG2023-231-01 and 2022d084).

Consent for publication

Not applicable.

Competing interests

Conflicts of interest are not asserted by the authors.

Author details

¹Biotherapy Center, The Third Affiliated Hospital, Sun Yat-sen University, Guangzhou 510630, Guangdong, PR China

²Department of Hepatic Surgery and Liver Transplantation Center, The Third Affiliated Hospital of Sun Yat-sen University, Guangzhou 510630, Guangdong, PR China

³Neurosurgery Department, The Third Affiliated Hospital of Sun Yat-sen University, Guangzhou 510630, Guangdong, PR China

⁴Vaccine Research Institute, The Third Affiliated Hospital of Sun Yat-sen University, Sun Yat-sen University, Guangzhou 510630, Guangdong, PR China

Received: 19 January 2024 / Accepted: 7 August 2024

Published online: 28 August 2024

References

- Saidi RF, Kenari SK. Liver ischemia/reperfusion injury: an overview [J]. *J Invest Surg.* 2014;27:366–79.
- Ikeda T, Yanaga K, Kishikawa K, et al. Ischemic injury in liver transplantation: difference in injury sites between warm and cold ischemia in rats [J]. *Hepatology.* 1992;16(2):454–61.
- Huet PM, Nagaoka MR, Desbiens G, et al. Sinusoidal endothelial cell and hepatocyte death following cold ischemia-warm reperfusion of the rat liver [J]. *Hepatology.* 2004;39(4):1110–9.
- Pine JK, Aldouri A, Young AL, et al. Liver transplantation following donation after cardiac death: an analysis using matched pairs [J]. *Liver Transpl.* 2009;15(9):1072–82.
- Serracino-Inglott F, Habib NA, Mathie RT. Hepatic ischemia-reperfusion injury [J]. *Am J Surg.* 2001;181:160–6.
- Nastos C, Kalimeris K, Papoutsidakis N, Tasoulis MK et al. Global consequences of liver ischemia/reperfusion injury [J]. *Oxid Med Cell Longev.* 2014;2014:906–965.
- Guo WA. The search for a magic bullet to fight multiple organ failure secondary to ischemia/reperfusion injury and abdominal compartment syndrome [J]. *J Surg Res.* 2013;184(2):792–3.
- Guo WZ, Fang HB, Cao S, et al. Sixtransmembrane epithelial antigen of the prostate 3 deficiency in hepatocytes protects the liver against ischemia-reperfusion injury by suppressing transforming growth factor- β -activated kinase 1 [J]. *Hepatology.* 2020;71:1037–54.
- Rampes S, Ma DQ. Hepatic ischemia-reperfusion injury in liver transplant setting: mechanisms and protective strategies [J]. *J Biomedical Res.* 2019;33(4):221–34.
- Fan Q, tao R, Zhang H, et al. Dectin-1 contributes to myocardial ischemia/reperfusion injury by regulating macrophage polarization and neutrophil infiltration [J]. *Circulation.* 2019;139:663–78.
- Hai Wang Z, Xi L, Deng, et al. Macrophage polarization and liver IschemiaReperfusion Injury [J]. *Int J Med Sci.* 2021;18:1104–13.
- Hanschen M, Zahler S, Krombach F, et al. Reciprocal activation between CD4+T cells and kupffer cells during hepatic ischemia-reperfusion [J]. *Transplantation.* 2008;86(5):710–8.
- Dal-Secco D, Wang J, Zeng Z, Kolaczowska E, et al. A dynamic spectrum of monocytes arising from the in situ reprogramming of CCR2+ monocytes at a site of sterile injury [J]. *J Exp Med.* 2015;212:447–56.
- Hopfner KP, Hornung V. Molecular mechanisms and cellular functions of cGAS-STING signalling [J]. *Nat Rev Mol Cell Biol.* 2020;21:501–21.
- Qin YF, Qiu DB, Zhang Q. HNF1A regulates the crosstalk between innate immune responses and MAFLD by mediating autophagic degradation of TBK1. *Autophagy.* 2023;19(3):1026–7.
- Li K, Gong YH, Qiu DB, et al. Hyperbaric oxygen facilitates Teniposide-induced cGAS-STING activation to enhance the anti-tumor efficacy of PD-1 antibody in HCC. *J Immunother Cancer.* 2022;10(8):e004006.
- He JY, Du C, Peng XY, Hong WL, et al. Hepatocyte nuclear factor 1A suppresses innate immune response by inducing degradation of TBK1 to inhibit steatohepatitis. *Genes Dis.* 2023;10(4):1596–612.
- Liu KP, Qiu DB, Liang X, et al. Lipotoxicity-induced STING1 activation stimulates MTORC1 and restricts hepatic lipophagy. *Autophagy.* 2022;18(4):860–76.
- Wang Z, Chen N, Li Z, et al. The cytosolic DNA-Sensing cGAS-STING pathway in Liver diseases. *Front Cell Dev Biol.* 2021;9:717610.
- Jiao J, Jiang Y, Qian Y, et al. Expression of STING is increased in monocyte-derived macrophages and contributes to liver inflammation in hepatic ischemia-reperfusion Injury. *Am J Pathol.* 2022;192(12):1745–62.
- Chen MX, Meng QC, Qin YF, et al. TRIM14 inhibits cGAS degradation mediated by selective autophagy receptor p62 to promote Innate Immune responses. *Mol Cell.* 2016;64(1):105–19.
- Wu XY, Chen YJ, Liu CA et al. STING induces Liver Ischemia-Reperfusion Injury by promoting calcium-dependent caspase 1-GSDMD Processing in macrophages. *Oxid Med Cell Longev.* 2022: 8123157.
- Zhan YQ, Xu DW, Tian YZ, et al. Novel role of macrophage TXNIP-mediated CYLD-NRF2-OASL1 axis in stress-induced liver inflammation and cell death. *JHEP Rep.* 2022;4(9):100532.
- Luo XJ, Li HG, Ma LQ, et al. Expression of STING is increased in liver tissues from patients with NAFLD and promotes macrophage-mediated hepatic inflammation and fibrosis in mice. *Gastroenterology.* 2018;155(6):1971–84.
- Yu YS, Liu Y, An WS, et al. STING-mediated inflammation in Kupffer cells contributes to progression of nonalcoholic steatohepatitis. *J Clin Invest.* 2019;129(2):546–55.
- Kozicky LK, Sly LM. Depletion and reconstitution of macrophages in mice. *Methods Mol Biol.* 2019;1960:101–12.
- Haag SM, Gulen MF, Raymond L, et al. Targeting STING with covalent small-molecule inhibitors. *Nature.* 2018;559(7713):269–73.
- Lama L, Adura C, Xie W, et al. Development of human cGAS-specific small-molecule inhibitors for repression of dsDNA-triggered interferon expression. *Nat Commun.* 2019;10(1):2261.
- Liu Y, Lu T, Zhang C, et al. Activation of YAP attenuates hepatic damage and fibrosis in liver ischemia-reperfusion injury. *J Hepatol.* 2019;71(4):719–30.
- Bardallo RG, Panisello-Roselló A, Sanchez-Nuno S, et al. Nrf2 and oxidative stress in liver ischemia/reperfusion injury. *FEBS J.* 2022;289(18):5463–79.
- Zhao M, Wang Y, Li L, et al. Mitochondrial ROS promote mitochondrial dysfunction and inflammation in ischemic acute kidney injury by disrupting TFAM-mediated mtDNA maintenance. *Theranostics.* 2021;11(4):1845–63.
- Li Y, Yang Q, Chen H, et al. TFAM downregulation promotes autophagy and ESCC survival through mtDNA stress-mediated STING pathway. *Oncogene.* 2022;41(30):3735–46.
- Yu Y, Liu Y, An W, et al. STING-mediated inflammation in Kupffer cells contributes to progression of nonalcoholic steatohepatitis. *J Clin Invest.* 2019;129(2):546–55.
- Chen L, Dong J, Liao S, et al. Loss of Sam50 in hepatocytes induces cardioprotein-dependent mitochondrial membrane remodeling to trigger mtDNA release and liver injury. *Hepatology.* 2022;76(5):1389–408.
- Liu Z, Wang M, Wang X, et al. XBP1 deficiency promotes hepatocyte pyroptosis by impairing mitophagy to activate mtDNA-cGAS-STING signaling in macrophages during acute liver injury. *Redox Biol.* 2022;52:102305.
- Xu Y, Chu C, Shi Z, et al. The role of hepatocyte mitochondrial DNA in liver injury. *Biomed Pharmacother.* 2023;168:115692.
- Xian HX, Watari K, Sanchez-Lopez E, et al. Oxidized DNA fragments exit mitochondria via mPTP- and VDAC-dependent channels to activate NLRP3 inflammasome and interferon signaling. *Immunity.* 2022;55:1–16.
- White MJ, McArthur K, Metcalf D, et al. Apoptotic caspases suppress mtDNA-induced STING-mediated type I IFN production. *Cell.* 2014;159(7):1549–62.
- Rongvaux A, Jackson R, Harman CCD, et al. Apoptotic caspases prevent the induction of type I interferons by mitochondrial DNA. *Cell.* 2014;159(7):1563–77.
- Wolf P, Schoeniger A, Edlich F. Pro-apoptotic complexes of BAX and BAK on the outer mitochondrial membrane. *Biochim Biophys Acta Mol Cell Res.* 2022;1869(10):119317.
- Singal AK, Guturu P, Hmoud B, et al. Evolving frequency and outcomes of liver transplantation based on etiology of liver disease [J]. *Transplantation.* 2013;95(5):755–60.
- Koh PO. Melatonin prevents hepatic injury-induced decrease in akt downstream targets phosphorylations [J]. *J Pineal Res.* 2011;51(2):214–9.
- Ding WX, Zhang Q, Dong YB, et al. Adiponectin protects the rats liver against chronic intermittent hypoxia induced injury through AMP-activated protein kinase pathway [J]. *Sci Rep.* 2016;6:34151.
- Yang WL, Chen J, Meng YH, et al. Novel targets for treating ischemia-reperfusion injury in the liver [J]. *Int J Mol Sci.* 2018;19(5):E1302.
- Ke B, Shen XD, Kamo N, et al. Beta-catenin regulates innate and adaptive immunity in Mouse Liver Ischemia-Reperfusion Injury. *Hepatology.* 2013;57:1203–14.

46. Yue S, Zhu J, Zhang M, et al. The myeloid heat shock transcription factor 1/ Beta-Catenin Axis regulates NLR Family, Pyrin Domain-containing 3 Inflammasome activation in Mouse Liver Ischemia/Reperfusion Injury. *Hepatology*. 2016;64:1683–98.
47. Maekawa H, Inoue T, Ouchi H, et al. Mitochondrial damage causes inflammation Via cGAS-STING Signaling in Acute kidney Injury. *Cell Rep*. 2019;29:1261–73.
48. Xu D, Chen L, Chen X, et al. The Triterpenoid CDDO-imidazole ameliorates Mouse Liver Ischemia-Reperfusion Injury through activating the Nrf2/HO-1 pathway enhanced Autophagy. *Cell Death Dis*. 2017;8:e2983.
49. West AP, Shadel GS. Mitochondrial DNA in Innate Immune responses and Inflammatory Pathology. *Nat Rev Immunol*. 2017;17:363–75.
50. Zhao B, Du F, Xu P, et al. A conserved PLPLRT/SD motif of STING mediates the recruitment and activation of TBK1. *Nature*. 2019;569:718–22.
51. Motwani M, Pesiridis S, Fitzgerald KA. DNA sensing by the cGAS-STING pathway in Health and Disease. *Nat Rev Genet*. 2019;20:657–74.
52. Wu J, Sun L, Chen X, et al. Cyclic GMP-AMP is an endogenous second Messenger in Innate Immune Signaling by cytosolic DNA. *Science*. 2013;339:826–30.
53. Lei Z, Deng M, Yi Z, et al. cGAS-mediated Autophagy protects the Liver from Ischemia-Reperfusion Injury independently of STING. *Am J Physiol Gastrointest Liver Physiol*. 2018;314:G655–667.
54. Shen A, Zheng D, Luo Y, et al. MicroRNA-24-3p alleviates hepatic ischemia and reperfusion injury in mice through the repression of STING signaling. *Biochem Biophys Res Commun*. 2020;522:47–52.
55. Zhong W, Rao Z, Rao J, et al. Aging aggravated liver ischemia and reperfusion injury by promoting STING-mediated NLRP3 activation in macrophages. *Aging Cell*. 2020;19:e13186.
56. Lai X, Gong J, Wang W, et al. Acetyl-3-aminoethyl salicylate ameliorates hepatic ischemia/reperfusion injury and liver graft survival through a high-mobility group box 1/toll-like receptor 4-dependent mechanism. *Liver Transpl*. 2019;25(8):1220–32.
57. Yue S, Zhu J, Zhang M, et al. The myeloid heat shock transcription factor 1/ beta-catenin axis regulates NLR family, pyrin domain-containing 3 inflammasome activation in mouse liver ischemia/ reperfusion injury. *Hepatology*. 2016;64(5):1683–98.
58. Nakahira K, Kyung SY, Rogers AJ, et al. Circulating mitochondrial DNA in patients in the ICU as a marker of mortality: derivation and validation. *PLoS Med*. 2013;10(12):e1001577.

Publisher's Note

Springer Nature remains neutral with regard to jurisdictional claims in published maps and institutional affiliations.